

# Few-Shot Segmentation with Global and Local Contrastive Learning

Weide Liu, Zhonghua Wu, Henghui Ding, Fayao Liu, Jie Lin and Guosheng Lin

**Abstract**—In this work, we address the challenging task of few-shot segmentation. Previous few-shot segmentation methods mainly employ the information of support images as guidance for query image segmentation. Although some works propose to build cross-reference between support and query images, their extraction of query information still depends on the support images. We here propose to extract the information from the query itself independently to benefit the few-shot segmentation task. To this end, we first propose a prior extractor to learn the query information from the unlabeled images with our proposed global-local contrastive learning. Then, we extract a set of predetermined priors via this prior extractor. With the obtained priors, we generate the prior region maps for query images, which locate the objects, as guidance to perform cross interaction with support features. In such a way, the extraction of query information is detached from the support branch, overcoming the limitation by support, and could obtain more informative query clues to achieve better interaction. Without bells and whistles, the proposed approach achieves new state-of-the-art performance for the few-shot segmentation task on PASCAL-5<sup>+</sup> and COCO datasets.

**Index Terms**—Few-shot Learning, Few-shot segmentation, prior extractor, constrastive learning.

## I. INTRODUCTION

SEMANtic segmentation is a fundamental task that classifies each pixel to a particular class. With the great success of deep learning, fully supervised semantic segmentation [1] has achieved remarkable achievements. However, fully supervised learning has some intrinsic limitations, such as it requires a large amount of pixel-level annotated image samples for model training. Moreover, abundant annotations for novel classes are required when we need to extend the current segmentation model to novel classes.

Few-shot segmentation is proposed to address the above issues by learning a network to predict segmentation masks

W. Liu is with School of Computer Science and Engineering, Nanyang Technological University (NTU), Singapore 639798 (e-mail: weide001@e.ntu.edu.sg).

Z. Wu is with School of Computer Science and Engineering, Nanyang Technological University (NTU), Singapore 639798 (e-mail: zhonghua001@e.ntu.edu.sg).

H. Ding is with School of Electrical and Electronic Engineering, Nanyang Technological University (NTU), Singapore 639798 (e-mail: ding0093@e.ntu.edu.sg).

F. Liu is with the Institute for Infocomm Research (I<sup>2</sup>R)-Agency for Science, Technology and Research (A\*star), Singapore, 138632 (e-mail: Liu\_Fayao@i2r.a-star.edu.sg).

J. Lin is with the Institute for Infocomm Research (I<sup>2</sup>R)-Agency for Science, Technology and Research (A\*star), Singapore, 138632 (e-mail: LinJ@i2r.a-star.edu.sg).

G. Lin is with School of Computer Science and Engineering, Nanyang Technological University (NTU), Singapore 639798 (e-mail: gslin@ntu.edu.sg).

Corresponding author: Guosheng Lin.

W. Liu and Z. Wu make equal contributions.

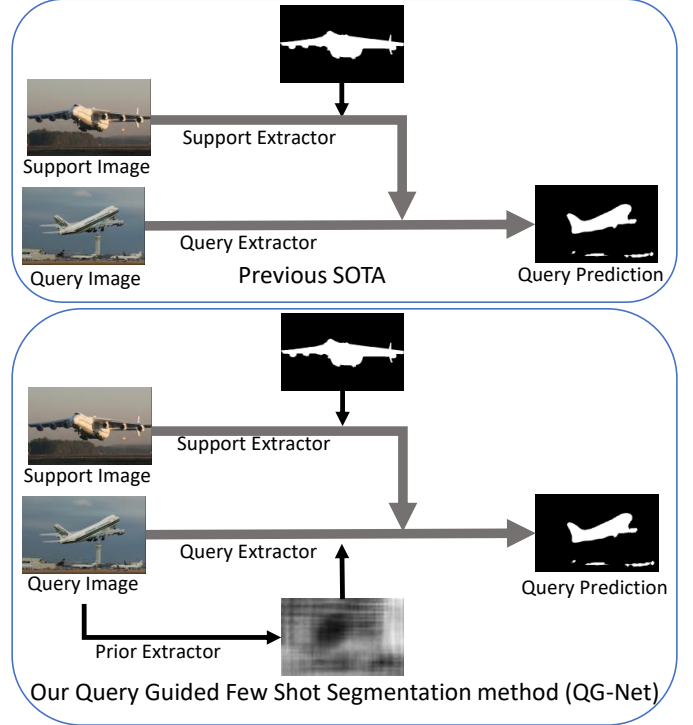


Fig. 1. Comparison between the pipeline of our proposed Query Guided Few Shot Segmentation method (QG-Net) with previous state-of-the-art (SOTA) few-shot segmentation methods. Previous works (upper part) only employ support images' information as guidance for query mask estimation, while our QGNet (lower part) utilizes the clues of query images with query extractor as guidance for final query mask prediction.

for the novel classes with only a few annotated novel classes training samples. Currently, state-of-the-art few-shot segmentation methods [2]–[5] utilize clues of support images to guide the query images segmentation with a two-branch architecture. However, they only employ support images' information as guidance for query masks prediction but do not discover clues of query images themselves. To utilize the query information, CRNet [6] proposes a cross-reference mechanism that enables the interaction between support and query image features. Similarly, prototype alignment regularization is used to align the query and support prototypes in PANet [3]. Though they build cross guidance between query and support images, those methods are limited to the labeled support images since all the information extraction/propagation, e.g., support-to-query and query-to-support, are essentially based on support masks. In this work, we argue that it is helpful to further detach

the query information extraction from support branch and generate query clues independently for enhancing few-shot segmentation performance and generalization. To this end, we propose a prior extractor to learn the query information from the unlabeled query images themselves with self-supervised learning.

One of the most promising directions among self-supervised learning methods is contrastive learning [7]. Images are first transformed into different variants. Contrastive loss is used to minimize the feature distances between the variants from the same images while maximizing the feature distances obtained from different images. Contrastive learning aims to step over the gap between the fully and less supervised classification via learning a predetermined prior of the objects without the labeled data. However, the current state-of-the-art design [8] is sub-optimal for segmentation tasks for the following reasons: 1) Image segmentation is a pixel-level classification task where both the local and global representations are essential, but [8] is only designed on image-level with global representation only. 2) There are usually multiple objects that co-existed in one image, *e.g.*, keyboard, desk, and computer, but the global contrastive loss cannot distinguish these different objects within the identical image. To address the above issues, we propose a predetermined prior learning method to obtain more distinguishable image features for the few-shot semantic segmentation task.

Specifically, we leverage the global and local contrastive loss to learn a prior extractor for few-shot image segmentation. A global contrastive loss is applied to the global representations to minimize the distance of features obtained by different variants of an identical image. To further distinguish different objects within the identical image, we divorce to get the local representations by splitting the image into local patches. Pixels in each patch contain similar features and contexts. We then apply a local contrastive loss between the local patches to learn a local predetermined prior. Similar to the global contrastive loss, the local contrastive loss targets to maximize the feature distance between different patches, *e.g.*, computer patches and keyboard patches. We use both global and local contrastive losses to train our prior extractor to use both advantages.

Using the self-supervised method mentioned above, we train a prior extractor from the unlabeled data to store the predetermined prior for query images. Then, we propose a new few-shot segmentation architecture, as shown in Figure 1, to retrieve the query category semantic segmentation information from the priors. The given query images are encoded with the prior extractor and a feature extractor to generate the prior features and the bridge features, respectively. We then locate the target objects by calculating the pixel-wise similarity maps between the prior and bridge features. In such a way, we obtain the prior region maps of the query images through their own information, overcoming the limitations mentioned above. The support images are encoded by the same feature extractor to be projected to the same feature space with the bridge features. We then build cross interactions between support and bridge features to enhance the segmentation performance.

Our main contributions can be summarized as follows:

- To the best of our knowledge, we are the first to utilize

self-supervised feature learning methods on unlabeled query images to benefit the few-shot segmentation task. Specifically, a prior extractor is proposed to generate prior region maps from the query image themselves to guide the final query mask prediction.

- A global and local contrastive loss is proposed to train the prior extractor, making contrastive learning more suitable for the few shot segmentation tasks. With our proposed global-local learning, the query branch independently extracts informative clues from the query image itself and greatly enhances the cross interaction between query and support.
- Our network achieves state-of-the-art performances on PASCAL VOC 2012, COCO datasets. Specifically, our method achieves significant performance gain (5.9% mean mIoU and 7.4% mean mIoU among 4 splits under 1-shot and 5-shot setting, respectively) on the large-scale COCO dataset over previous SOTA.

## II. RELATED WORK

### A. Fully Supervised Semantic Segmentation

Semantic segmentation is a fundamental computer vision task, which aims to predict each pixel with a predefined class. Fully convolutional networks (FCN) [1] has been widely used in current state-of-the-art methods. Encoder-decoder [6], [9]–[16] is a popular structure used to reconstruct the high-resolution prediction map for semantic segmentation prediction. The encoder gradually downsamples the feature maps to obtain a large field-of-view, and the decoder recovers the fine-grained information. To keep the resolution of the feature maps not too small, dilated convolution [10] aims to increase the field-of-view without decreasing the feature map size and not increasing the number of the parameters. In our network, we also follow the encoder-decoder structure with a dilated convolution to generate the query segmentation masks.

### B. Few-shot Segmentation

Two-branch network architecture has been widely used in few-shot segmentation tasks. Previous works [2], [4], [4]–[6], [17]–[25] encode the labeled support images into category features to guide the query mask prediction. However, these works only employ support images' information as guidance for query images but do not discover clues of query images themselves. To improve the efficiency of using the query image information, CRNet [6] proposes a cross-reference mechanism to enable the query and support image interaction for better model training. PANet [3] also proposed a prototype alignment network to guide both query and support image segmentation. However, even those methods align both support and query clues and guide each other; the query mask prediction is still limited to the labeled support images since their information extraction of query images still depends on support. In this work, we argue that using unlabeled query images to train an image prior extractor could benefit the query segmentation mask prediction.

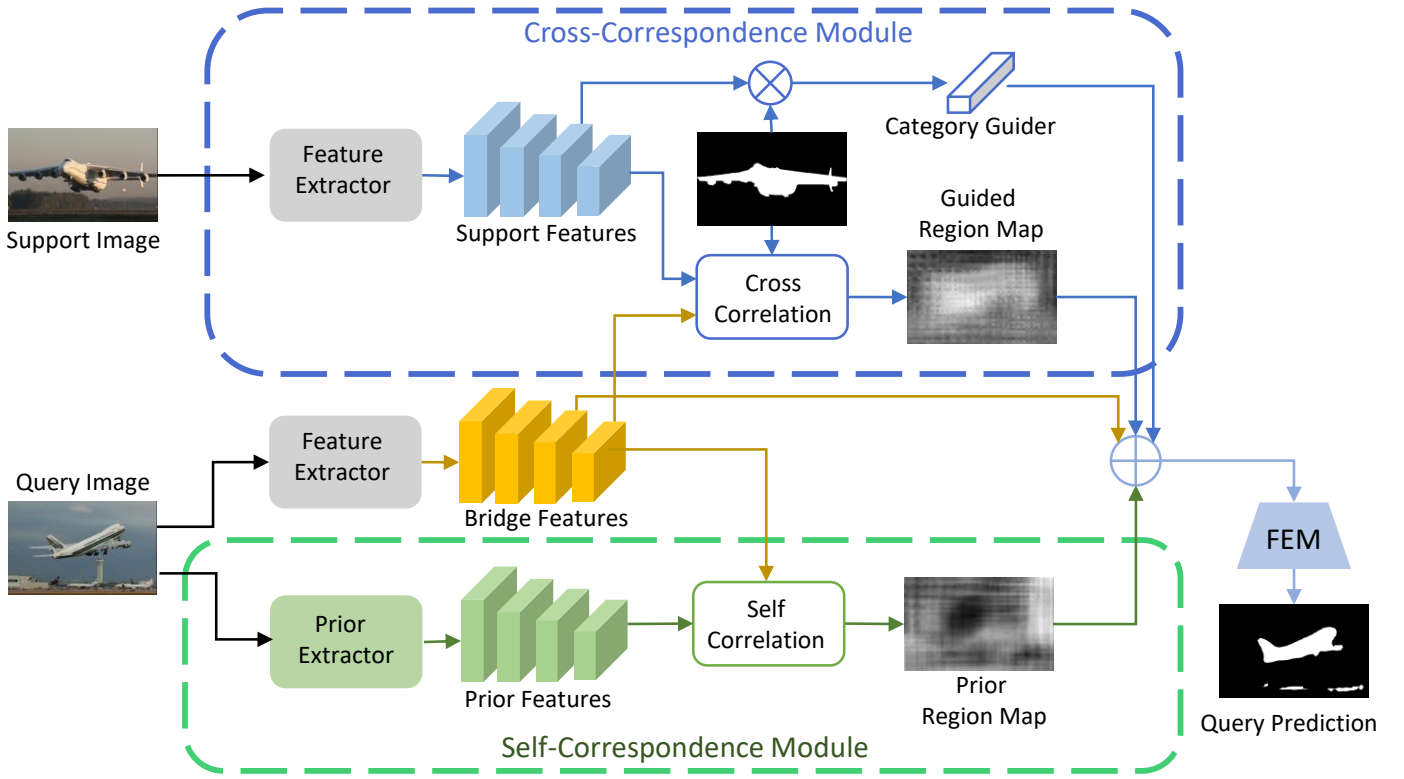


Fig. 2. Our proposed method consists of a self-correspondence module and a cross-correspondence module. Unlike the previous SOTA, a self-correspondence module (green) is proposed to extract prior features and generate a prior region map to locate the target object regions from the query image itself. A Cross-correspondence module (blue) is proposed to generate a guided region map to identify the query object region with the category guide from the masked support feature. Finally, the prior region map and guided region map are concatenated with category and bridge features for the final query mask prediction (FEM).

### C. Contrastive learning

Currently, self-supervised contrastive learning methods [8], [26] have been widely used in computer vision tasks to learn a feature extractor from unlabeled images as pre-training for other downstream tasks. The contrastive learning methods aim to pulling close the representations of different views of the same image and pushing away the representations of different images. SimCLR [27] proposes a simple framework for self-supervised learning by applying contrastive learning to representations of the same image with different data augmentation. MoCo [8], [28] increases the negative memory bank size with a moving average network (momentum encoder). This paper also utilizes contrastive learning to learn a prior extractor from the unlabeled query images to benefit the few shot segmentation task.

### III. TASK DEFINITION

Few-shot semantic segmentation aims to perform segmentation with only a few annotated examples on novel classes. We divide the images into two sets, the target images called query set  $\mathcal{Q}$  and the annotated images serve as support set  $\mathcal{S}$ . Provided  $K$  annotated samples from the support set, the model aims to predict binary masks for the query images, while the annotated support images should provide the foreground

categories. The categories in the training image set have no overlap with the test image set.

Given a network  $\mathcal{R}_\theta$  parameterized by  $\theta$ , in each episode, we first sample a target category  $c$  from the dataset  $\mathcal{C}$ . Based on the sampled classes, we then collect  $K + 1$  labeled images  $\{(x_s^1, y_s^1), (x_s^2, y_s^2), \dots, (x_s^K, y_s^K), (x_q, y_q)\}$  from the dataset, which contains at least one object belongs to the sampled category  $c$ . Among them, we sample  $K$  labeled images constitute the support set  $\mathcal{S}$ , and the last one is served as the query set  $\mathcal{Q}$ . After that, we make predictions on the query images by inputting the support set and the query image into the model  $\hat{y}_q = \mathcal{R}_\theta(\mathcal{S}, x_q)$ . At training time, we learn the model parameters  $\theta$  by optimizing the cross-entropy loss  $\mathcal{L}(\hat{y}_q, y_q)$ , and repeat such procedures until convergence.

### IV. METHOD

Few shot semantic segmentation task aims to learn a network to predict the novel classes with only a few annotated data. Most of the previous works [2], [4]–[6], [24] solve the few shot tasks by learning a network with the annotated support images. Unlike previous works limited to support images, we aim to discover clues of query images from themselves to benefit the query mask prediction. As shown in Figure 2, the proposed method consists of two main modules: the self-correspondence module and the cross-correspondence

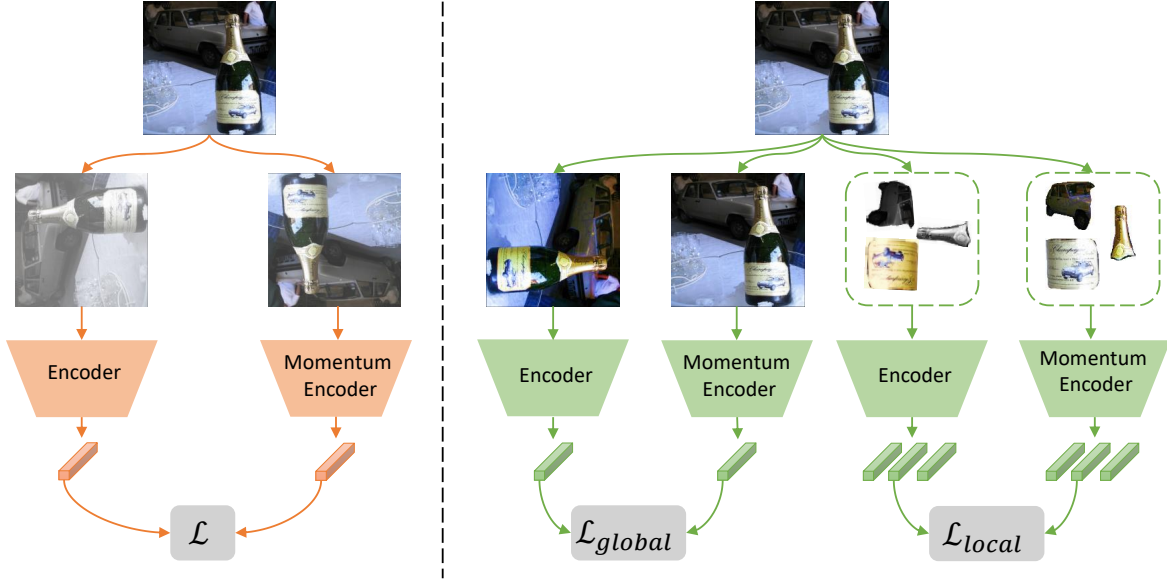


Fig. 3. The difference between conventional contrastive learning and our proposed global-local contrastive learning. Conventional contrastive learning methods (left) only learn contrast from a global perspective. Our global-local contrastive learning learns the contrast with two additional local patches as input and builds a contrastive loss across the global and local representation.

module. In the self-correspondence module, we firstly train a prior extractor from the unlabeled query images with our proposed global and local contrastive losses to store the prior features. With the prior features, we aim to propagate the stored prior information to the bridge features to obtain the object regions as our prior region maps. Meanwhile, the cross-correspondence module is utilized to generate a guided region map and the category guider to determine the query category information with the annotated support images for final query masks prediction.

This section first briefly introduces the global contrastive loss to teach the model to distinguish the dissimilar image features. Then we will introduce our proposed local contrastive loss, which aims to distinguish different object patches. To be noticed, the quality of the patches is one critical influencing factor for our local contrastive learning, which is important for our prior features generation. We analyze different ways to generate the patches and apply them to calculate the local contrastive loss and optimize the prior extractor. Next, we introduce the generation of prior region map and guided region map from our pretrained prior extractor and feature extractor. Finally, we analyze an interesting discovery: the prior region maps have a low correspondence value at the object regions. In contrast, the conventional guided region maps have a high correspondence value at the object regions.

#### A. Prior Extractor

1) *Global Contrastive Learning*: The global contrastive loss [7] has been widely used for pre-training by distinguishing features obtained from different images. In this paper, we also use the global contrastive loss to learn a global level prior to distinguish the image level features.

Following [28], we random sample one image from the dataset and transform the image into two different variants

as a positive pair. For the negative pairs  $I_k$ , we sample one image from the queue. Consider we encode one query image  $I_q$  to vector  $q$ , and encode a set of reference images (negative pairs) as keys to vectors  $k_{0,1,\dots}$ . We use the InfoNCE [29] as our contrastive loss:

$$\mathcal{L}_{global} = -\log \frac{\exp(q \cdot k_+ / \tau)}{\sum_{i=0}^K \exp(q \cdot k_i / \tau)}. \quad (1)$$

Here we set  $K = 65536$  to get  $K$  negative samples,  $k_+$  is the positive pair from the same image, and the  $\tau$  is a temperature hyper-parameter [30]. The value of the contrastive loss is low when the feature similarity is high for positive pairs and low for negative pairs.

We follow MoCo [8] to build a dynamic dictionary to keep a large dictionary size. The dictionary's keys will be updated by replacing the oldest mini-batch with the new one following a momentum way [8].

2) *Local Contrastive Learning*: The global contrastive loss aims to learn a global-prior feature by teaching the model to distinguish dissimilar images. However, several limitations still exist on applying global contrastive loss for segmentation task pre-training, 1) The global contrastive loss only discriminates the dissimilar image, regardless of different objects within one image. 2) The common co-existing instances might result in a negative effect with only global contrastive loss. *e.g.*, the keyboard and the computer usually appear in the same image. However, usually, we need to segment them into different classes.

In this paper, we propose a local contrastive loss to distinguish different objects in order to benefit the few-shot segmentation task. We segment the images into local patches and pre-train the model by applying the local contrastive loss on the patches. We first introduce how we generate the patches



with different methods. Then we will show how to use the patches to serve the few shot segmentation tasks.

**Patch generation method 1: Felzenszwalb's efficient graph based segmentation.** To guarantee that the generated patches align with the same semantic categories, follow [31], we segment the images by assigning the local patches with the same contexts. As shown in algorithm 1, at first, we build an undirected graph  $G = (V, E)$ , the initial elements  $v_i$  in  $V$  are pixels, the edges  $E$  are the edges connecting the pixels. The weight  $w$  of the edges is the dissimilarity of two pixels connected by the edge. We define the weight of edge  $e_{i,j}$  with their pixel intensity  $w_{i,j} = I_i - I_j$ . In the beginning, we treat each pixel as a component and merge the components connected with low weight as one component until all the edges have been calculated.  $MInt(C_i, C_j)$  is the internal different in the components  $C_i$  and  $C_j$ . Each final component serves as a local patch for our prior generation.

---

**Algorithm 1** Generate local patches with Felzenszwalb's efficient graph based segmentation [31]

---

Input: One image  
Output:  $S = (C_1, C_2, \dots, C_r)$   
Initialization: We build an undirected graph based on the image color  $G = (V, E)$  with  $n$  vertices and  $m$  edges, where  $v_i \in V$ ,  $V$  denotes the image pixels,  $e \in E$ ,  $E$  denotes the correspondences of the neighboring vertices, and  $w$  denotes the weight of  $e$ .  
Sort the edge  $E$  with their edge weight.  
 $S^0$ : Where each  $v_i$  is each pixel.  
**for**  $q = 1, 2, \dots, m$  **do**  
    Construct  $S^q$  based on  $S^{q-1}$   
    Let  $o_q = (v_i, v_j)$   
    Let  $v_i \in C_i$  and  $v_j \in C_j$   
    **if**  $C_i^{q-1} \neq C_j^{q-1}$  and  $w(o_q) \leq MInt(C_i^{q-1}, C_j^{q-1})$  **then**  
         $S^q = S^{q-1} \cup C_i^{q-1} \cup C_j^{q-1}$   
    **else**  
         $S^q = S^{q-1}$   
    **end if**  
**end for**

---

**Patch generation method 2: Simple Linear Iterative Clustering (SLIC).** We generate the image patches by clustering pixels based on their color similarity and proximity in the image plane. Follow [32], we fuse both the color and position information of each pixel into a five dimensions format ( $labxy$ ). Here  $lab$  denotes the color information and  $xy$  denotes the spatial position. To cluster the 5D spaces pixels, new distance measures between pixels need to be used. As shown in Algorithm 2, for every input image, we choose  $K$  cluster centers  $C_k$  with regular grid intervals  $S = \sqrt[N/K]{N}$ , where  $N$  denotes the number of pixel of the input image. We assume that the cluster center connects to the associated pixels within a  $2S \times 2S$ . We calculate the 5D distance ( $D_s$ ) between the pixels  $k, i$  with the following equation:

$$D_s = D_{lab} + D_{xy}/S \times m. \quad (2)$$

In the equation 2,  $D_{lab}$  denotes the color distance and  $D_{xy}$

denotes the spatial distance:

$$D_{lab} = \sqrt{((l_k - l_i)^2 + (a_k - a_i)^2 + (b_k - b_i)^2)}, \quad (3)$$

$$D_{xy} = \sqrt{((x_k - x_i)^2 + (y_k - y_i)^2)}. \quad (4)$$

In equation 2, we normalize the spatial distance by dividing the interval  $S$  and the variable  $m$  aims to control the compactness of the superpixel.

We re-center the cluster center to the lowest gradient position within  $n \times n$  distance to the existing center (we choose  $n = 3$ ) for every cluster center. The gradient generated with :

$$G_{xy} = ||I(x+1, y) - I(x-1, y)||^2 + ||I(x, y+1) - I(x, y-1)||^2. \quad (5)$$

Where  $x, y$  denotes the pixel positional and the  $I_{x,y}$  denotes the corresponding color feature vector—each pixel connected to its nearest cluster center within the search distance. Furthermore, a new center is generated by averaging all the pixels within the same cluster. The process of associating pixels with the nearest cluster center and re-center the cluster is repeated until convergence. When there remain unconnected pixels  $E$  less than the *threshold*, we enforce them to connect to the largest neighboring cluster and stop the process of clustering. Each superpixel (cluster) serves as a local patch for our prior generation.

---

**Algorithm 2** Generate local patches with Simple Linear Iterative Clustering

---

Initialize cluster centers  $C_k = [C_1, C_2, C_3, \dots]$  with a grid distance  $S$   
Re-center the cluster within  $3 \times 3$  regions to the lowest gradient position with equation 5  
**repeat**  
    **for** Each cluster **do**  
        Assign the pixels to the cluster with the distance measure in equation 2  
    **end for**  
    Compute new cluster centers and residual error  $E$ .  
**until**  $E \leq \text{threshold}$   
**return** Each cluster

---

**Local contrastive loss.** We aim to distinguish the patches by applying the local contrastive loss on the patches generated with the above methods. Consider we random sample one query patch and encoder it to  $q_p$ , and a set of reference patches as our reference patches key,  $k_{p0, p1, \dots}$ . A local contrastive loss aims to minimize the distance between similar patches and maximize the distance between dissimilar patches. So our local contrastive loss should be:

$$\mathcal{L}_{local} = -\log \frac{\exp(q_p \cdot k_p + \tau)}{\sum_{i=0}^M \exp(q_p \cdot k_{pi} / \tau)}. \quad (6)$$

Here, we keep  $M = 65536$  negative sample patches in the queue, and the  $k_p$  is the positive patch pairs with different views from the same patch, the  $k_{pi}$  denotes the negative patch pairs, and the  $\tau$  is a temperature hyper-parameter [30].

We use both local and global contrastive loss to generate our query prior:

$$\mathcal{L} = \mathcal{L}_{local} + \mathcal{L}_{global}. \quad (7)$$

### B. Generate region maps for few-shot segmentation tasks

As shown in Figure 2, in this section, we show how to generate the prior region map and guided region map from our pretrained prior extractor and the feature extractor to benefit the few-shot segmentation tasks.

We set  $I_q$  denotes the query images,  $I_s$  denotes the support images, and  $M_s$  denotes the support annotations.  $F_p$  denotes our pretrained prior extractor, and  $F$  denotes the feature extractor. We encode the images with:

$$X_q = F(I_q), X_s = F(I_s), P_q = F_p(I_q). \quad (8)$$

1) *Generate prior region maps:* For every query image, we retrieve the query information from our prior features by calculating the correlation between the bridge features  $X_q$  and  $P_q$ . Specifically, we generate the prior region maps with the following steps: we first calculate the pixel-wise cosine similarity  $\cos(x_q, p_{q'})$  between the the bridge feature  $x_q \in X_q$ , and the prior feature  $p_{q'} \in P_q$ :

$$\cos(x_q, p_{q'}) = \frac{x_q^T p_{q'}}{\|x_q\| \|p_{q'}\|}. \quad (9)$$

where  $q, q' \in \{1, 2, 3, \dots, hw\}$  and  $h, w$  denote the feature size. For the prior region map, we locate the object by define the confident background with the maximum similarity value alone the all prior features and combine them as the similarity map:

$$s_q = \max_{q' \in \{1, 2, \dots, hw\}} (\cos(x_q, p_{q'})), \quad (10)$$

$$S_Q = [s_1, s_2, \dots, s_{hw}]. \quad (11)$$

We normalize the correspondence value to  $(0, 1)$  with:

$$S_Q = \frac{S_Q - \min(S_Q)}{\max(S_Q) - \min(S_Q) + \epsilon}. \quad (12)$$

where  $\epsilon$  is set to  $1e-7$  in our experiments. Finally, we reshape  $S_Q$  into  $h \times w \times 1$  to the same size as our final prior region map to locate the objects.

2) *Generate guided region maps:* Follow the same step as IV-B1, we generate the guided region maps with the support features  $X_s$  and bridge features  $X_q$  within the cross-correspondence module. We filter out the irrelevant support features by multiplying the support features with the annotated support mask  $M_s \times X_s$ . In this way, the bridge feature pixels yield no correspondence with the background and only correlate with the target object area. We locate the confident query object regions by taking the maximum cosine similarity for each bridge feature among all the filtered support features.

Finally, we fuse prior and guided region map as our final correspondence maps to guide our network predictions. Combine the bridge features and the category guider, we adapt FEM [5] as a decoder to generate our final query masks.

### C. Opposite Region Maps

As shown in Figure 5, we discover that the prior region map generated by bridge features and prior features has a low correspondence value at the object regions while has a high value at the background regions. Our conjecture is that the prior learns the object features from the unlabeled images and store the information within the prior. The learned object features have been transferred to a new feature space, which is dissimilar to the features generated from the bridge encoder. However, the irrelevant objects (e.g., the background) remain in a similar feature space, which indicates high similarity to the features from the bridge encoder. So the prior region maps locate the target objects with the low similarity value. On the other hand, the support feature and bridge feature stay in the same feature space and are generated by different images; a high similarity score indicates high confidence that the regions contain similar objects.

## V. EXPERIMENT

### A. Implementation details

We use SGD as the optimizer with InfoNCE [29] loss to train the prior extractor. Following MOCO-v2 [28], we apply blur augmentation, color distortion, random crop, and random flip as the data augmentation methods. All the images in the dataset are used to train the prior extractor with 1000 epoch for the PASCAL VOC dataset and 200 epochs for the COCO dataset.

For few-shot segmentation model training, following previous methods [2]–[6], we choose different backbone (Resnet101, Resnet50, and VGG) and different image input size for a fair comparison. Similar to previous works [2], [5], [6], we adapt the dilated ResNet as the backbone to encode the feature in order to keep the feature resolution. We use SGD as the optimizer to train the network. Random crop, random scale, and random flip are using as the data augmentation methods during the training process.

If there are no special instructions, we conduct the experiments with Resnet-50 backbone and  $473 \times 437$  training image size.

### B. Datasets and Evaluation Metric

**PASCAL VOC 2012.** PASCAL-5<sup>i</sup> [37] contains 20 categories with 10582 images for training, 1449 images for validation, and 1456 for testing. For a fair comparison with previous works, we divide the dataset into training and testing sets following [5]. We divide the 20 object categories into 4 folds for the cross-validation experiments: three for training and one for testing. We train our network with 200 epochs with an initial learning rate of 0.0025 and a batch size of 4.

**MS COCO.** One limitation of PASCAL-5<sup>i</sup> is that it only involves 20 categories, which is insufficient to verify the model's capabilities on the few shot segmentation tasks. We also conduct cross-validation experiments on the large-scale MS COCO dataset, containing more categories and images to verify the model's capabilities on the few shot segmentation tasks. COCO 2014 [38] contains 80 object categories with

TABLE I

1-SHOT AND 5-SHOT mIoU RESULTS ON PASCAL-5<sup>i</sup> DATASET. THE TRAINING SIZE AND BACKBONE USED BY EACH METHOD ARE LISTED. OUR QGNET OUTPERFORMS THE STATE-OF-THE-ART UNDER ALL THE EXPERIMENT SETTINGS. THE RESULTS REPORTED WITH mIoU(%)

Methods	Training Size	Backbone	1-shot					5 shot				
			Fold-0	Fold-1	Fold-2	Fold-3	Mean	Fold-0	Fold-1	Fold-2	Fold-3	Mean
OSLSM [33]	-	VGG 16	33.6	55.3	40.9	33.5	40.8	35.9	58.1	42.7	39.1	43.9
co-FCN [19]	-	VGG 16	36.7	50.6	44.9	32.4	41.1	37.5	50.0	44.1	33.9	41.4
AMP-2 [22]	-	VGG 16	41.9	50.2	46.7	34.7	43.4	40.3	55.3	49.9	40.1	46.4
PFENet [5]	473 × 473	VGG 16	42.3	58.0	51.1	41.2	48.1	51.8	64.6	59.8	46.5	55.7
PANet [3]	417 × 417	VGG 16	42.3	58.0	51.1	41.2	48.1	51.8	64.6	59.8	46.5	55.7
FWBF [34]	512 × 512	VGG 16	47.0	59.6	52.6	48.3	51.9	50.9	62.9	56.5	50.1	55.1
Ours	321 × 321	VGG 16	52.9	65.0	50.7	51.6	55.0	56.8	67.3	51.2	58.2	58.3
Ours	473 × 473	VGG 16	58.6	67.2	52.3	52.0	57.5	58.7	68.4	52.6	55.0	58.7
CANet [2]	321 × 321	ResNet 50	52.5	65.9	51.3	51.9	55.4	55.5	67.8	51.9	53.2	57.1
PGNet [35]	321 × 321	ResNet 50	56.0	66.9	50.6	50.4	56.0	54.9	67.4	51.8	53.0	56.8
CRNet [6]	321 × 321	ResNet 50	-	-	-	-	55.7	-	-	-	-	58.8
PMMs [24]	321 × 321	ResNet 50	55.2	66.9	52.6	50.7	56.3	56.3	67.3	54.5	51.0	57.3
PPNet [4]	417 × 417	ResNet 50	47.8	58.8	53.8	45.6	51.5	58.4	67.8	64.9	56.7	62.0
PANet [3]	417 × 417	ResNet 50	44.0	57.5	50.8	44.0	49.1	55.3	67.2	61.3	53.2	59.3
PFENet [5]	473 X 473	ResNet 50	61.7	69.5	55.4	56.3	60.8	63.1	70.7	55.8	57.9	61.9
Ours	321 × 321	ResNet 50	57.9	67.2	52.4	55.5	58.2	59.2	69.4	53.0	64.5	61.5
Ours	473 × 473	ResNet 50	63.4	69.4	55.1	58.4	61.6	64.7	71.0	53.6	61.6	62.8
FWBF [34]	512 × 512	ResNet 101	51.3	64.5	56.7	52.2	56.2	54.8	67.4	62.2	55.3	59.9
PPNet [4]	417 × 417	ResNet 101	52.7	62.8	57.4	47.7	55.2	60.3	70.0	69.4	60.7	65.1
DAN [36]	-	ResNet 101	54.7	68.6	57.8	51.6	58.2	57.9	69.0	60.1	54.9	60.5
PFENet [5]	473 X 473	ResNet 101	60.5	69.4	54.4	55.9	60.1	62.8	70.4	54.9	57.6	61.4
Ours	321 × 321	ResNet 101	57.6	67.5	53.0	53.6	57.9	58.6	66.5	53.3	53.6	58.0
Ours	473 X 473	ResNet 101	60.3	69.3	53.3	57.4	60.1	67.6	71.8	55.1	64.4	64.7

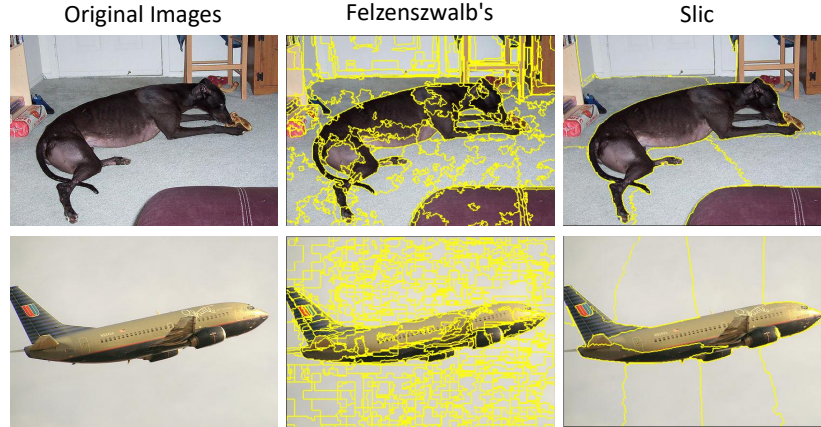


Fig. 4. Visualization of the local patches generated by Felzenszwalb's [31] method and the Slic [32]

82783 training images and 40504 validation images. Following PFENet [5], we evenly split the 80 categories into 4 folds. We use three folds for the model training and the other fold for testing.

**Evaluation Metric.** In previous works, there exist two evaluation metrics. Shaban *et al.* [33] report the results with the standard mean Intersection-Over-Union(mIoU). While [17], [19] ignore the categories and report the results by averaging of foreground IoU and background IoU (FBIOU). Following the previous works [2], [5], [33], we choose the standard mIoU as our evaluation metric with the following reasons: 1) The unbalanced image distribution (*e.g.*, in VOC test dataset, class sheep contains 49 images while the class person contains

378 images). 2) The score of the background IoU is very high for small objects, which will fail to evaluate the model's capability. Nevertheless, we still compare the previous state-of-the-art methods with both evaluation metrics. The evaluation metrics are calculated as follows:

$$IoU = \frac{Intersection}{Union} = \frac{TP}{TP + FP + FN}, \quad (13)$$

$$mIoU = \frac{1}{n} \sum_{i=1}^n (IoU_n), \quad (14)$$

$$FBIOU = \frac{1}{2} (IoU_{fg} + IoU_{bg}). \quad (15)$$



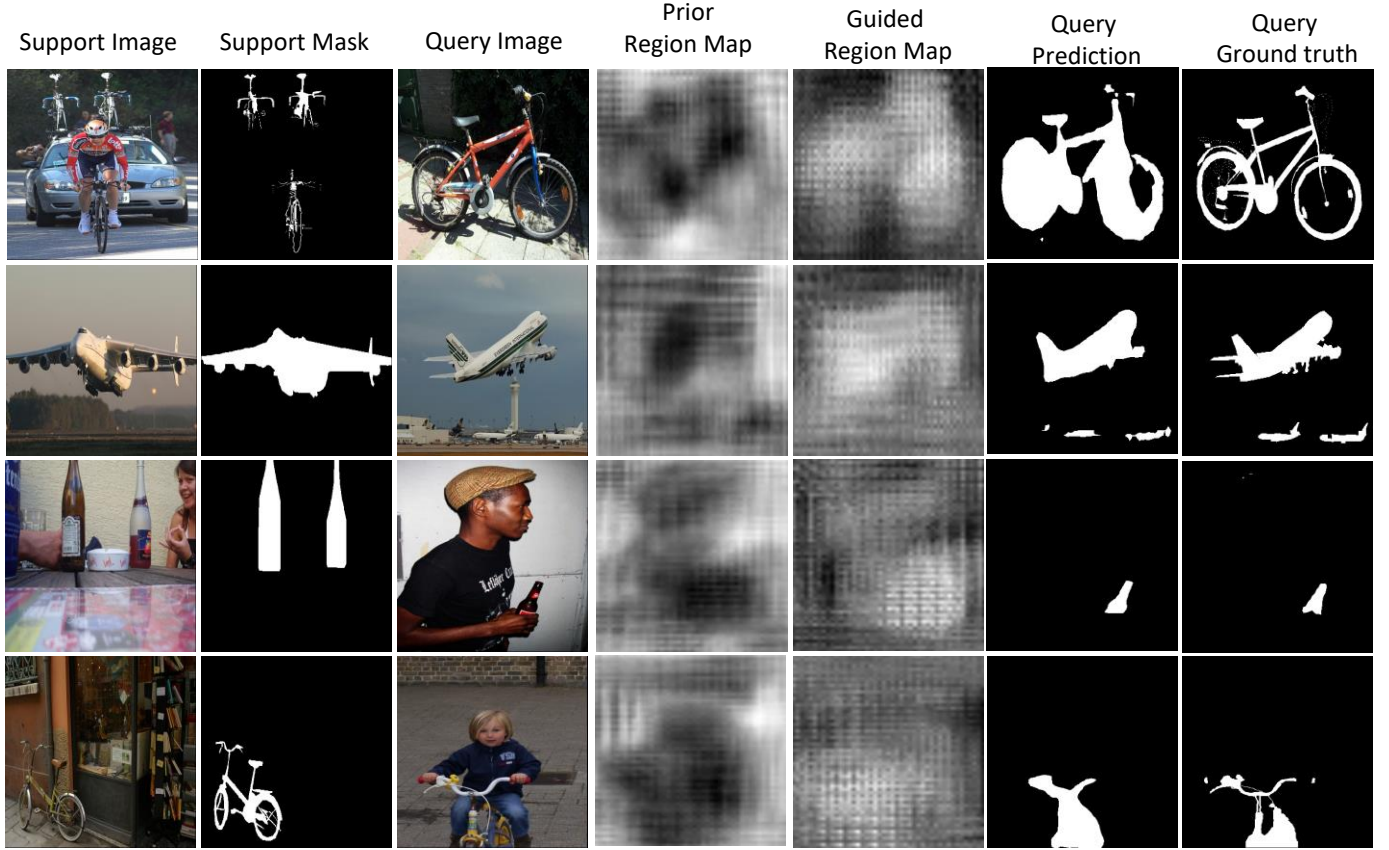


Fig. 5. Visualization results for guided region map, prior region map, and the query prediction generated by our proposed QGNet on PASCAL-5<sup>i</sup> dataset.

TABLE II  
COMPARISON WITH THE STATE-OF-THE-ART METHODS UNDER THE 1-SHOT AND 5-SHOT SETTING. THE RESULTS REPORTED ON PASCAL VOC 2012 DATASET WITH FBIOU(%).

Methods	1-shot (%)	5-shot (%)
OSLM [33]	61.3	61.5
co-fcn [19]	60.9	60.2
sg-one [21]	63.1	65.9
R-DFCN [20]	60.9	66.0
PL [17]	61.2	62.3
A-MCG [25]	61.2	62.2
CANet [2]	66.2	69.6
CRNet [6]	66.8	71.5
Ours	<b>72.2</b>	<b>73.9</b>

The TP denotes true positive, FP denotes false positive, FN denotes false negative,  $n$  denotes the classes' number. The standard mIoU is calculated by averaging the IoU of all classes. The  $IoU_{fg}$  is calculated with equation 13, which ignores the object categories, and  $IoU_{bg}$  is calculated in the same way but reversed the foreground and background. FBIOU average the  $IoU_{fg}$  and the  $IoU_{bg}$ .

### C. Comparisons with state-of-the-art

**PASCAL VOC 2012.** Different backbone and different training image sizes will have a huge impact on the final performance. To be fair to compare to previous SOA methods, we implement our method with different backbones (VGG16, Resnet50, Resnet101) and image size ( $321 \times 321$  and  $473 \times$

473). Table I shows the mIoU results of different methods on the PASCAL-5<sup>i</sup> dataset. As shown, our proposed method achieves the best results with different backbones and image sizes.

**MS COCO.** We compare our results with previous state-of-the-art methods under the standard mIoU in Table III. For the experiments on the large-scale MS COCO dataset, PFENet uses the image size of  $641 \times 641$  with ResNet-101 as the backbone to train the network. However, due to the GPU memory restriction, we still use the training size of  $473 \times 473$  and  $321 \times 321$  with ResNet-50 backbone to train the model. Despite this, our proposed QGNet is still able to achieve state-of-the-art results. We outperform previous SOTA PFENet by 5.9% and 7.4% in 1-shot and 5-shot settings, respectively.

In addition, we visualize some testing results on fold 0 of the PASCAL-5<sup>i</sup> dataset in Figure 5 and some testing results on the COCO dataset in Figure 6.

### D. Ablation studies

The key novelty of our method lies in the self-correspondence module, where we generate a prior region map for the query images independently. We firstly conduct ablation experiments to show the effectiveness of our proposed global and local contrastive losses for prior extractor training. Then we conduct experiments to find the best way for local patch generation during our local contrastive loss training. To further analyze how the prior region maps generated from the



TABLE III

1-SHOT AND 5-SHOT mIoU RESULTS ON COCO DATASET. THE RESULTS OF CANET\* IS OBTAINED FROM [24]. THE RESULTS REPORTED WITH mIoU(%)

Methods	Training Size	Backbone	1-shot					5 shot				
			Fold-0	Fold-1	Fold-2	Fold-3	Mean	Fold-0	Fold-1	Fold-2	Fold-3	Mean
PANet [3]	417 × 417	VGG 16	-	-	-	-	20.9	-	-	-	-	29.7
FWBF [34]	512 × 512	VGG 16	18.4	16.7	19.6	25.4	20.0	20.9	19.2	21.9	28.4	22.6
PFENet	473 × 473	VGG 16	33.4	36.0	34.1	32.8	34.1	35.9	40.7	38.1	36.1	37.7
CANet* [2]	321 × 321	ResNet 50	25.1	30.3	24.5	24.7	26.1	26.0	32.4	26.1	27.0	27.9
PMMs [24]	321 × 321	ResNet 50	29.5	36.8	29.0	27.0	30.6	33.8	42.0	33.0	33.3	35.5
PPNet [4]	-	ResNet 50	28.1	30.8	29.5	27.7	29.0	39.0	40.8	37.1	37.3	38.5
RPMM [24]	321 × 321	ResNet 50	29.5	36.8	28.9	27.0	30.6	33.8	42.0	33.0	33.3	35.5
PFENet [5]	473 × 473	ResNet 50	36.5	38.6	34.5	33.8	35.8	36.5	43.3	37.8	38.4	39.0
DAN [36]	-	ResNet 101	-	-	-	-	24.4	-	-	-	-	29.6
FWBF [34]	512 × 512	ResNet 101	19.9	18.0	21.0	28.9	21.2	19.1	21.5	23.9	30.1	23.7
PFENet [5]	641 × 641	ResNet 101	34.3	33.0	32.3	30.1	32.4	38.5	38.6	38.2	34.3	37.4
Ous	321 X 321	ResNet 50	34.4	38.5	34.6	33.2	35.2	38.9	46.2	39.1	38.9	40.7
Ours	473 × 473	ResNet 50	<b>36.7</b>	<b>41.4</b>	<b>38.7</b>	<b>36.6</b>	<b>38.3</b>	<b>41.5</b>	<b>48.1</b>	<b>46.3</b>	<b>43.6</b>	<b>44.8</b>

TABLE IV

COMPARISON WITH THE STATE-OF-THE-ART METHODS UNDER THE 1-SHOT AND 5-SHOT SETTING. OUR PROPOSED NETWORK OUTPERFORMS ALL PREVIOUS METHODS AND ACHIEVES NEW STATE-OF-THE-ART PERFORMANCE. THE RESULTS REPORTED ON MS COCO DATASET WITH FBIOU(%).

Method	1-shot (%)	5-shot (%)
PANet [3]	59.2	63.5
A-MCG [25]	52.0	54.7
PFENet [5]	58.6	61.9
DAN [36]	62.3	63.9
Ours	<b>62.4</b>	<b>66.2</b>

TABLE V

ABLATION STUDIES ON PASCAL-5<sup>i</sup> DATASET ABOUT THE TRAINING EPOCHS AND THE LOCAL PATCH GENERATION METHODS FOR PRIOR EXTRACTOR TRAINING. THE RESULTS REPORTED WITH mIoU(%)

Methods	Number of Epochs	1 shot				
		fold 0	fold 1	fold 2	fold 3	mean
Felzenszwalb [31]	1000	62.6	68.9	54.9	56.7	60.8
Felzenszwalb [31]	2000	62.7	69.3	54.7	56.8	60.9
Slic [32]	1000	63.4	69.4	55.1	58.4	61.6
Slic [32]	2000	62.4	69.4	55.2	57.0	61.0

query images affect the query mask prediction, we discuss the overlap between prior region maps and the guided region maps.

**Prior Extractor Training.** We conduct ablation experiments to analyze which patch generation method gives better

TABLE VI

ABLATION STUDIES ON PASCAL-5<sup>i</sup> DATASET ABOUT GLOBAL AND LOCAL CONTRASTIVE LEARNING. THE RESULTS REPORTED WITH mIoU(%)

Contrastive learning type:		1 shot				
local	global	fold 0	fold 1	fold 2	fold 3	mean
✓		63.2	69.3	54.9	57.4	61.2
	✓	62.2	69.7	54.5	57.5	60.9
✓	✓	63.4	69.4	55.1	58.4	61.6

performance for prior extractor training. Table V shows that we achieve better query mask prediction when we use Slic [32] as the patches generation method. As shown in Figure 4, the patches generated by Slic are larger than Felzenszwalb's method, and each patch is likely capturing one pattern of an object. We conjecture that a suitable patch size could benefit the prior extractor learning a more discriminative predetermined prior.

Table V also shows that 1000 epochs for prior extractor training with the Slic method yield the best performance.

**Effectiveness of global and local contrastive losses.** We conduct ablation experiments to show the effectiveness of our proposed global and local contrastive losses. Table VI shows that using both global and local contrastive losses gives the best performance. This suggests that global and local contrastive losses could help prior extractor store more discriminative prior for query mask prediction.

**Recall for region maps.** We further conduct ablation experiments to show the recall ability of guided region map and prior region map with groundtruth query segmentation mask. We define the object regions  $R$  With a threshold  $\alpha$ ,

$$R = \begin{cases} 1, & \text{if } V(x, y) > \alpha, \\ 0, & \text{otherwise.} \end{cases} \quad (16)$$

$V$  denotes the normalized values of the feature map.

The recall of the region maps with groundtruth mask is calculated as  $Recall = (R \cap R_{GT}) / R_{GT}$ . Here  $R_{GT}$  indicate the groundtruth mask region.  $Recall$  denotes the overlap between region map and groundtruth mask divided by the groundtruth mask. The higher the  $Recall$ , the more object regions of the region map can cover the groundtruth mask. In Table VII, the recall of the prior region map (denoted as  $Recall_{p,gt}$ ) is larger than the recall of the guided region map (denoted as  $Recall_{g,gt}$ ), which suggests that the prior region map could cover more potential object regions.

TABLE VII  
ABLATION STUDIES ON PASCAL-5<sup>i</sup> FOLD-0 DATASET ABOUT THE RECALL FOR GUIDED REGION MAP AND PRIOR REGION MAP WITH GROUND TRUTH QUERY MASK. THE RESULTS REPORTED WITH mIoU(%)

threshold	0.1	0.2	0.3	0.4	0.5	0.6	0.7	0.8	0.9
$Recall_{g,gt}$	99.9%	99.9%	99.3%	96.0%	85.6%	65.6%	39.6%	15.5%	2.2%
$Recall_{p,gt}$	99.9%	99.9%	99.1%	96.5%	89.7%	76.2%	54.7%	28.2%	6.6%

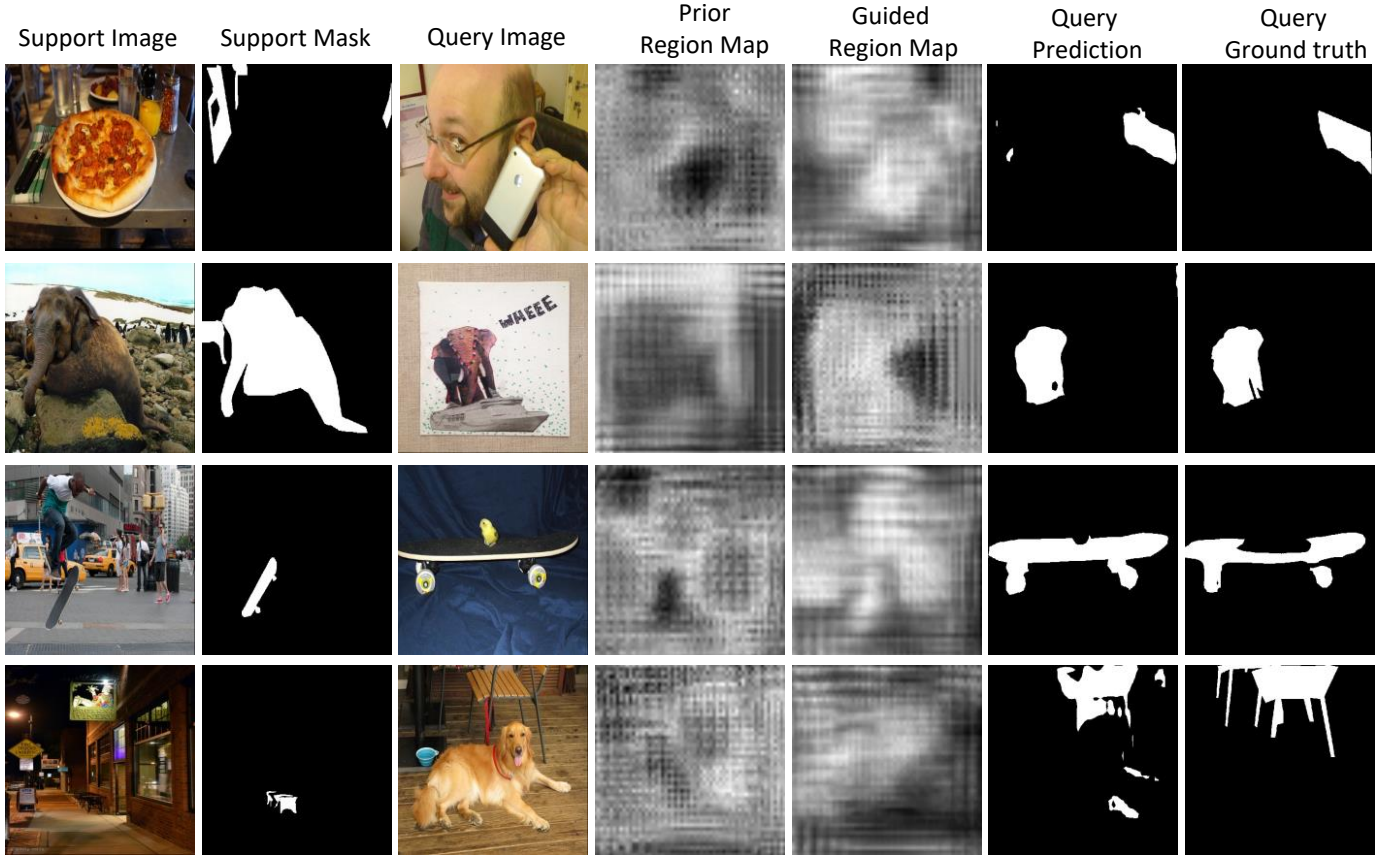


Fig. 6. Visualization results for guided region map, prior region map, and the query prediction generated by our proposed QGNet on COCO dataset.

### E. Failure case analysis

In this section, we analyze the challenging cases that fail our model on the COCO dataset. As shown in Figure 7, our model fails to distinguish between the people and Teddy bear, horse and person. This is because they have a similar pattern or similar color: difficult to distinguish without semantic information. Moreover, our model can not locate small objects. When the query information is too complex, our model can only identify the small part of the human being.

## VI. CONCLUSION

This paper has proposed the Query Guided Few Shot Segmentation method (QG-Net) to learn the query information from the unlabeled image with self-supervised learning. Specifically, we proposed a global-local contrastive loss to train the prior extractor, making the query branch independently extract informative clues from the query image and greatly enhancing the cross interaction between query and support. The performances on PASCAL VOC 2012 and MS

COCO dataset validate our methods and achieve new state-of-the-art.

## REFERENCES

- [1] J. Long, E. Shelhamer, and T. Darrell, "Fully convolutional networks for semantic segmentation," in *Proceedings of the IEEE conference on computer vision and pattern recognition*, 2015, pp. 3431–3440. 1, 2
- [2] C. Zhang, G. Lin, F. Liu, R. Yao, and C. Shen, "Canet: Class-agnostic segmentation networks with iterative refinement and attentive few-shot learning," in *Proceedings of the IEEE Conference on Computer Vision and Pattern Recognition*, 2019, pp. 5217–5226. 1, 2, 3, 6, 7, 8, 9
- [3] K. Wang, J. H. Liew, Y. Zou, D. Zhou, and J. Feng, "Panet: Few-shot image semantic segmentation with prototype alignment," in *Proceedings of the IEEE International Conference on Computer Vision*, 2019, pp. 9197–9206. 1, 2, 6, 7, 9
- [4] Y. Liu, X. Zhang, S. Zhang, and X. He, "Part-aware prototype network for few-shot semantic segmentation," in *European Conference on Computer Vision*. Springer, 2020, pp. 142–158. 1, 2, 3, 6, 7, 9
- [5] Z. Tian, H. Zhao, M. Shu, Z. Yang, R. Li, and J. Jia, "Prior guided feature enrichment network for few-shot segmentation," *TPAMI*, 2020. 1, 2, 3, 6, 7, 9
- [6] W. Liu, C. Zhang, G. Lin, and F. Liu, "Crnet: Cross-reference networks for few-shot segmentation," in *Proceedings of the IEEE/CVF Conference*

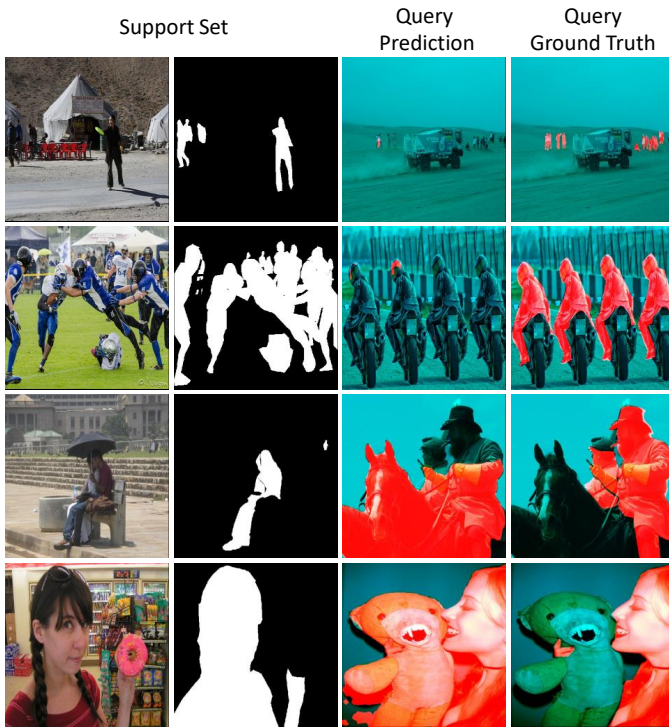


Fig. 7. The failure cases on COCO dataset.

- on Computer Vision and Pattern Recognition, 2020, pp. 4165–4173. 1, 2, 3, 6, 7, 8
- [7] R. Hadsell, S. Chopra, and Y. LeCun, “Dimensionality reduction by learning an invariant mapping,” in *2006 IEEE Computer Society Conference on Computer Vision and Pattern Recognition (CVPR’06)*, vol. 2. IEEE, 2006, pp. 1735–1742. 2, 4
- [8] K. He, H. Fan, Y. Wu, S. Xie, and R. Girshick, “Momentum contrast for unsupervised visual representation learning,” in *Proceedings of the IEEE/CVF Conference on Computer Vision and Pattern Recognition*, 2020, pp. 9729–9738. 2, 3, 4
- [9] G. Lin, F. Liu, A. Milan, C. Shen, and I. Reid, “Refinenet: Multi-path refinement networks for dense prediction,” *IEEE transactions on pattern analysis and machine intelligence*, vol. 42, no. 5, pp. 1228–1242, 2019. 2
- [10] L.-C. Chen, G. Papandreou, I. Kokkinos, K. Murphy, and A. L. Yuille, “Deeplab: Semantic image segmentation with deep convolutional nets, atrous convolution, and fully connected crfs,” *IEEE transactions on pattern analysis and machine intelligence*, vol. 40, no. 4, pp. 834–848, 2018. 2
- [11] H. Ding, X. Jiang, B. Shuai, A. Q. Liu, and G. Wang, “Semantic segmentation with context encoding and multi-path decoding,” *IEEE Transactions on Image Processing*, vol. 29, pp. 3520–3533, 2020. 2
- [12] S. Zhou, D. Nie, E. Adeli, J. Yin, J. Lian, and D. Shen, “High-resolution encoder-decoder networks for low-contrast medical image segmentation,” *IEEE Transactions on Image Processing*, vol. 29, pp. 461–475, 2019. 2
- [13] Z. Huang, C. Wang, X. Wang, W. Liu, and J. Wang, “Semantic image segmentation by scale-adaptive networks,” *IEEE Transactions on Image Processing*, vol. 29, no. 1, pp. 2066–2077, 2019. 2
- [14] L. Yang, J. Han, D. Zhang, N. Liu, and D. Zhang, “Segmentation in weakly labeled videos via a semantic ranking and optical warping network,” *IEEE Transactions on Image Processing*, vol. 27, no. 8, pp. 4025–4037, 2018. 2
- [15] B. Shuai, H. Ding, T. Liu, G. Wang, and X. Jiang, “Toward achieving robust low-level and high-level scene parsing,” *IEEE Transactions on Image Processing*, vol. 28, no. 3, pp. 1378–1390, 2018. 2
- [16] L. Jing, Y. Chen, and Y. Tian, “Coarse-to-fine semantic segmentation from image-level labels,” *IEEE Transactions on Image Processing*, vol. 29, pp. 225–236, 2019. 2
- [17] N. Dong and E. Xing, “Few-shot semantic segmentation with prototype learning,” in *BMVC*, 2018. 2, 7, 8
- [18] X. Li, T. Wei, Y. P. Chen, Y.-W. Tai, and C.-K. Tang, “Fss-1000: A 1000-class dataset for few-shot segmentation,” in *Proceedings of the IEEE/CVF Conference on Computer Vision and Pattern Recognition*, 2020, pp. 2869–2878. 2
- [19] K. Rakelly, E. Shelhamer, T. Darrell, A. Efros, and S. Levine, “Conditional networks for few-shot semantic segmentation,” in *ICLR Workshop*, 2018. 2, 7, 8
- [20] M. Siam and B. Oreshkin, “Adaptive masked weight imprinting for few-shot segmentation,” *arXiv preprint arXiv:1902.11123*, 2019. 2, 8
- [21] X. Zhang, Y. Wei, Y. Yang, and T. Huang, “Sg-one: Similarity guidance network for one-shot semantic segmentation,” *arXiv preprint arXiv:1810.09091*, 2018. 2, 8
- [22] M. Siam, B. N. Oreshkin, and M. Jagersand, “Amp: Adaptive masked proxies for few-shot segmentation,” in *Proceedings of the IEEE International Conference on Computer Vision*, 2019, pp. 5249–5258. 2, 7
- [23] Z. Dong, R. Zhang, X. Shao, and H. Zhou, “Multi-scale discriminative location-aware network for few-shot semantic segmentation,” in *2019 IEEE 43rd Annual Computer Software and Applications Conference (COMPSAC)*, vol. 2. IEEE, 2019, pp. 42–47. 2
- [24] B. Yang, C. Liu, B. Li, J. Jiao, and Q. Ye, “Prototype mixture models for few-shot semantic segmentation,” *arXiv preprint arXiv:2008.03898*, 2020. 2, 3, 7, 9
- [25] T. Hu, P. Yang, C. Zhang, G. Yu, Y. Mu, and C. G. Snoek, “Attention-based multi-context guiding for few-shot semantic segmentation,” 2019. 2, 8, 9
- [26] J.-B. Grill, F. Strub, F. Altché, C. Tallec, P. H. Richemond, E. Buchatskaya, C. Doersch, B. A. Pires, Z. D. Guo, M. G. Azar *et al.*, “Bootstrap your own latent: A new approach to self-supervised learning,” *arXiv preprint arXiv:2006.07733*, 2020. 3
- [27] T. Chen, S. Kornblith, M. Norouzi, and G. Hinton, “A simple framework for contrastive learning of visual representations,” in *International conference on machine learning*. PMLR, 2020, pp. 1597–1607. 3
- [28] X. Chen, H. Fan, R. Girshick, and K. He, “Improved baselines with momentum contrastive learning,” *arXiv preprint arXiv:2003.04297*, 2020. 3, 4, 6
- [29] A. v. d. Oord, Y. Li, and O. Vinyals, “Representation learning with contrastive predictive coding,” *arXiv preprint arXiv:1807.03748*, 2018. 4, 6
- [30] Z. Wu, Y. Xiong, S. X. Yu, and D. Lin, “Unsupervised feature learning via non-parametric instance discrimination,” in *Proceedings of the IEEE Conference on Computer Vision and Pattern Recognition*, 2018, pp. 3733–3742. 4, 5
- [31] P. F. Felzenszwalb and D. P. Huttenlocher, “Efficient graph-based image segmentation,” *International journal of computer vision*, vol. 59, no. 2, pp. 167–181, 2004. 5, 7, 9
- [32] R. Achanta, A. Shaji, K. Smith, A. Lucchi, P. Fua, and S. Süsstrunk, “Slic superpixels compared to state-of-the-art superpixel methods,” *IEEE transactions on pattern analysis and machine intelligence*, vol. 34, no. 11, pp. 2274–2282, 2012. 5, 7, 9
- [33] A. Shaban, S. Bansal, Z. Liu, I. Essa, and B. Boots, “One-shot learning for semantic segmentation,” *arXiv preprint arXiv:1709.03410*, 2017. 7, 8
- [34] K. Nguyen and S. Todorovic, “Feature weighting and boosting for few-shot segmentation,” in *Proceedings of the IEEE International Conference on Computer Vision*, 2019, pp. 622–631. 7, 9
- [35] C. Zhang, G. Lin, F. Liu, J. Guo, Q. Wu, and R. Yao, “Pyramid graph networks with connection attentions for region-based one-shot semantic segmentation,” in *Proceedings of the IEEE International Conference on Computer Vision*, 2019, pp. 9587–9595. 7
- [36] H. Wang, X. Zhang, Y. Hu, Y. Yang, X. Cao, and X. Zhen, “Few-shot semantic segmentation with democratic attention networks,” 7, 9
- [37] M. Everingham, L. Van Gool, C. K. Williams, J. Winn, and A. Zisserman, “The pascal visual object classes (voc) challenge,” *International journal of computer vision*, vol. 88, no. 2, pp. 303–338, 2010. 6
- [38] T.-Y. Lin, M. Maire, S. Belongie, J. Hays, P. Perona, D. Ramanan, P. Dollár, and C. L. Zitnick, “Microsoft coco: Common objects in context,” in *ECCV*, 2014, pp. 740–755. 6